TÜBİTAK

Turkish Journal of Chemistry

http://journals.tubitak.gov.tr/chem/

Research Article

Turk J Chem
(2018) 42: 1720 – 1735
© TÜBİTAK
doi:10.3906/kim-1806-71

Optimization of sugarcane bagasse activation to achieve adsorbent with high affinity towards phenol

Seyed-Abolfazl MOHTASHAMI[1], **Neda ASASIAN KOLUR**[2,*], **Tahereh KAGHAZCHI**[1], **Reza ASADI-KESHEH**[1], **Mansooreh SOLEIMANI**[1]

[1]Department of Chemical Engineering, Amirkabir University of Technology, Tehran, Iran
[2]Fouman Faculty of Engineering, College of Engineering, University of Tehran, Fouman, Iran

Received: 30.06.2018 • **Accepted/Published Online:** 10.09.2018 • **Final Version:** 06.12.2018

Abstract: Sugarcane bagasse as an agricultural/industrial biomass was converted into a low-cost activated carbon via an acid activation procedure under optimized conditions. Phosphoric acid was applied as a cost-effective and environmentally friendly chemical activator. The optimized activated carbon produced under temperature of 550 °C and impregnation ratio of 1.5 showed a micromesoporous structure with specific surface area and pore volume of 972.5 m^2/g and 0.43 cm^3/g, respectively. The adsorption capacity of the produced AC towards phenol was measured and, after only 30 min, the removal percentage reached over 95%. The greatest affinity towards phenol was obtained at pH of 4 justified by the pH_{pzc} of the sorbent and speciation of phenol in solution. Under the intermediate concentration range, the Dubinin–Radushkevich isotherm was the best-fit model for describing the equilibrium data. The apparent adsorption energy was equal to 10.94 kJ/mol. All the evidence showed that the mechanisms involved in phenol adsorption were ion-exchange, electrostatic, and physical adsorption.

Key words: Phenol, adsorption, sugarcane bagasse, activated carbon, Taguchi

1. Introduction

The final cost of adsorbents is one of the key challenges in using adsorption processes, especially for treating wastewaters. Owing to the limited accessibility and high price of original carbonaceous sources (coal and wood) for activated carbon production, the interest in converting low-cost biomass wastes into nonconventional adsorbents is increasing.[1] Another advantage is no necessity of recovery of saturated forms of these sorbents. Around the world, huge volumes of agricultural wastes such as nut shells, rice husk, bagasse pith, and sawdust wastes are accessible at no cost. Handling wastes with such large volumes may cause additional costs for industrial and agricultural units. Environmental difficulties including polluted run-off water and the probability of creating fire and explosion risks (particularly for bagasse waste stacks) are other drawbacks of waste disposal. Iran is a country with vast land under sugarcane cultivation with bagasse production of about 8% of the worldwide production per year.[2] Therefore, a large amount of sugarcane bagasse waste is produced annually in this country, making it a good choice for developing carbonaceous adsorbents.

Conversion of bagasse into activated carbon (AC) can be carried out via chemical activation, physical activation, or a hybrid of these approaches.[3–6] Chemical activation is preferred in many works because of the simplicity, higher rate of activation under moderate operating conditions, and high production yields.[7] Among

*Correspondence: n.asasian@ut.ac.ir

the various chemical agents used for activation of cellulosic materials, phosphoric acid has several advantages compared to KOH, $ZnCl_2$, etc. H_3PO_4 is affordable, ecofriendly, and easily recoverable; it can also be recycled back into the process.[7,8] Some of the studies that investigated the chemical activation of sugarcane bagasse using phosphoric acid are as follows: Satyawali and Balakrishnan applied acid impregnation (with sulfuric, phosphoric, nitric, and hydrochloric acids) at a ratio of 4:3 at 150 °C for 12 h together with thermal activation (at 500 °C for 1 h) or separately to produce AC from bagasse and other agricultural residues. Among the chemicals, phosphoric acid as a good dehydrating agent showed the most successful performance in bagasse activation (BET surface area of 492 m^2/g).[9] Soleimani and Kaghazchi also evaluated chemical activation of bagasse wastes using phosphoric acid. They found that the ultimate activation temperature, time, heating rate, and impregnation ratio are the important factors in determining the quality of activated carbon.[10] Giraldo-Gutierrez and Moreno-Pirajan also succeeded in obtaining an adsorbent from bagasse by applying combined chemical/physical activation procedures. After bagasse pyrolysis at 700 °C for 2 h under N_2 atmosphere, milled and sieved chars were soaked for 10 min in a HNO_3 solution (30%); the final step was CO_2 activation at 900 °C for 4 h. These researchers produced another AC sample through a simple chemical activation procedure involving impregnation with H_3PO_4 solution (2 h) and then heating under inert atmosphere at 900 °C for 2 h. The BET surface areas achieved by these two methods were respectively equal to 260 and 320 m^2/g. In addition, chemical treatment with phosphoric acid generated higher amounts of acid groups on the carbon surface.[11] Elwakeel et al. also prepared AC with 671.5 m^2/g BET surface area and iodine value of 602.2 mg/g through chemical activation of sugarcane bagasse using H_3PO_4 at 500 °C for 2 h with production yield of about 27%.[12] In the investigation performed by Adib et al., the influence of phosphoric acid concentration (5% to 30%) on the characteristics of bagasse-based AC was studied. According to that work, bagasse activated with H_3PO_4 (30%) showed the optimal bulk density (0.3023 g/cm^3), ash content (4.35%), iodine adsorption capacity (974.96 mg/g), and pore size (0.21–0.41 µm).[13] Based on the satisfying efficiency of H_3PO_4, this material was considered as the chemical activator for activation of sugarcane bagasse in the present work.

H_3PO_4-activated sugarcane bagasse has been applied for removal of several kinds of pollutants/solutes from aqueous systems, including different types of dyes, [14] gold,[15] Fe(II) and Mn(II),[12] and o-toluidine and benzidine;[16] however, to the best of our knowledge, no published paper is available on the application of this kind of AC for adsorption of phenolic compounds. Phenol is one of the most carcinogenic and toxic aromatic compounds with maximum allowed concentration of 1 ppm for effluent discharge to surface waters and use in agricultural and irrigating purposes based on the Iranian Department of Environment. Its toxic character is enhanced after chlorination of water and conversion into chlorophenol. Many industrial activities including coke ovens, coal conversion, phenolic resin production, and fiberglass manufacturing are the main sources of phenolic compounds with significant concentrations of phenol (up to 7000 ppm) in wastewaters. Petroleum refineries and textile units produce wastewaters with relatively smaller phenol contents in the range of 40–200 ppm. Other plants such as leather, ferrous materials and rubber, pulp and paper, and paint industries have much lower phenol in wastewaters (1–10 ppm).[17] Among the different promising treatment methods, the most economic and effective method for treating wastewaters containing relatively low phenol concentrations is adsorption onto the various kinds of porous adsorbents including commercial activated carbons, natural wastes and their activated forms, synthetic polymers, and clays.[18]

Many researchers used raw bagasse or its chemically treated forms (not activated) as biosorbents for phenol removal,[19] and in several works, bagasse fly ash was applied. For example, Gupta et al. used bagasse

fly ash for adsorption of phenol and p-nitrophenol from aqueous systems,[20] and Srivastava et al. investigated the adsorption behavior of bagasse fly ash towards phenol in both batch and column modes. Bagasse fly ash is a waste collected from the flue gas of sugarcane-bagasse-fired boilers without any further activation.[21,22] Only in a few works was phenol removal performed using chemically and physically activated sugarcane bagasse. For example, Karunarathne and Amarasinghe investigated the fixed bed adsorption of phenol by an activated carbon sample that was prepared by thermal activation of sugarcane bagasse at 600 °C in the absence of air. The produced adsorbent was the carbonized bagasse, not the activated form.[23] Mukherjee et al. produced a carbonaceous adsorbent by burning sugarcane waste at 900 °C for 8 h. The posttreatment activation was done by mixing the bagasse ash with hot distilled water and then soaking in 1 N HNO_3 solution for 24 h at room temperature.[24] In another work, Kalderis et al. activated sugarcane bagasse by $ZnCl_2$ impregnation and then carbonization at 700 °C in a rotary furnace, and then applied it for phenol adsorption.[25] That is the work most similar to the current research; however, the chemical agents used were different. Therefore, the use of H_3PO_4-activated sugarcane bagasse for phenol adsorption can be considered as the novelty of this work.

The present work has concentrated on the application of phosphoric acid activated sugarcane bagasse for phenol removal. The Taguchi procedure and L_9 inner arrays were applied to design the adsorbent preparation and adsorption experiments; the iodine number and equilibrium adsorption capacity towards phenol were respectively the criteria to select the optimal activation and adsorption conditions. Additionally, characterization of the adsorbent was performed for determination of the chemical, physical, and porous properties of activated carbons.

2. Results and discussion

2.1. Adsorbent production results

The Taguchi design of the experiments performing 9 runs under predetermined conditions showed that achieving the adsorbent with the highest affinity towards iodine (680 mg I_2/g) is possible under the following conditions: impregnation ratio = 1.5 wt./wt.; activation temperature = 550 °C, and time = 1 h. The predicted iodine number deviated from the corresponding experimental value by only 1%. The analysis of variance (ANOVA) data related to the activation of bagasse are given in Table 1. The ANOVA indicated the impregnation ratio as the most influencing factor on the iodine number with a contribution of ~60.2%. After that, temperature and time of activation were second and third most influential, respectively, with percentages of ~36.4% and 2.6%. The negligible influence of activation time on the iodine number indicated that there is no significant preference between 0.5 and 2 h; however, it was set as 1 h for the final tests considering both economic issues and effectiveness. The small increase in the error percentage (only about 6%) after ignoring the factor (time) confirmed its negligible role. The Fisher ratio (or F test) in the ANOVA table showed which factors significantly affected the process response. This was carried out by comparison of the calculated F values with the corresponding F values in Fisher tables available for different accuracies.[26] According to Table 1, all the factors have statistically significant influences on the iodine number (>90% and 99.99% significance).

Figure 1a shows that both impregnation ratio and temperature of activation have increasing effects on the iodine number and adsorptive properties of ACs over the ranges studied. The impregnation ratio of 0.25 weakly contributes in formation of fine pores and fractures. However, increasing the value up to 0.75 developed the porous structure of raw bagasse significantly; the increasing trend continued up to 1.5 but with a much smaller slope. It was established that at low concentrations H_3PO_4 usually results in micropore development, and higher concentrations lead to increasing mesopores.[27] The results obtained by Castro et al. also confirmed

Table 1. Results of the analysis of the variance (ANOVA table) for AC production.

Factor	DOF* (f)	Sum of squares (S)	Variance (V)	F-ratio (F)	Significance	Percent (%)
Impregnation ratio	2	87449.273	43724.636	296.829	>99.99%	60.226
Activation temperature	2	52950.731	26475.365	179.73	>99.99%	36.386
Activation time	2	4017.79	2008.895	13.637	>90.00%	2.572
Other/error	2	294.611	147.305			0.816
Total	8	144712.407				100.00%

*DOF: Degrees of freedom.

the trend; they investigated the effect of impregnation ratio in the range of 1 to 2.5 on the BET surface area of adsorbent and found that the best amount to reach the highest surface area was 1.5.[14] The loss of the adsorptive properties at impregnation ratios higher than 1.5 can be attributed to the presence of excess chemicals leading to too much increase in the volume of mesopores, combining them and probably converting them into macropores. Similar behavior was observed for increasing the activation temperature between 350 and 550 °C. The weakest performance was related to 350 °C because of the insufficient energy for activation and reaction of chemical agents with cellulosic structure. Higher temperature seems to be more suitable for activation. Castro el al. also reported the temperature of 500 °C as the best temperature for activation of sugarcane bagasse in the presence of H_3PO_4. They found that the activated carbon produced at lower temperatures (300 °C) had very limited microporous structure. The surface area is developed at higher temperatures because of the development of larger pores. However, temperatures of 600 °C and higher decrease the total pore volume because of the contraction of the carbon structure, combination of micropores, and heat shrinkage.[14,28] Other researchers also preferred the temperature of 500 °C to activate sugarcane bagasse with H_3PO_4.[4,12,29] In spite of the slight influence on the activation efficiency, increasing the activation time from 0.5 to 1 h resulted in creating and developing porosity (Figure 1a). In contrast, continuing the process for 2 h had a destructive influence on the porosity of the adsorbent, maybe because of the interconnection of fine pores and conversion of them into large macropores. Similar ascending-descending results were also obtained by Castro et al. Shorter activation times than 1 h were not enough for full development of porosity, and prolongation of activation time led to the breakdown of the cross-links within the carbon structures and too much pore widening.[14]

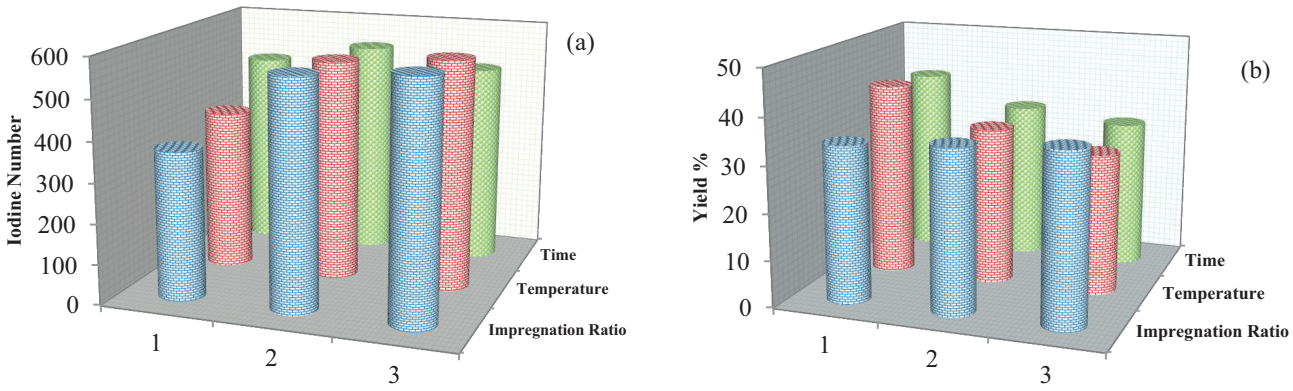

Figure 1. The influence of activation parameters on (a) the iodine number and (b) activation yield of the bagasse-based ACs: 1, 2, and 3 represent the corresponding levels of each parameter in the Taguchi design.

One of the benefits of applying the Taguchi design for experiments is the capability of the procedure to predict the interactions between various factors. Interaction is the failure of one factor to produce the same influence on the response at diverse levels of another variable.[30] The interaction severity index (SI) predicted by the Taguchi method is defined to measure the angle between two straight lines in an interaction plot (between two 2-level factors); the angle, ranging between 0° and 90°, is expressed on a scale of 0–100 as the SI.[30] In the present work, SI values were calculated for each pair of factors (Figure 2). A relatively high interaction was observed between time and two other factors (temperature and impregnation ratio); however, the SI between the impregnation ratio and temperature of activation was smaller (about 12.75). This means that the influence of temperature (or impregnation ratio) on the response is significantly under the influence of time; however, temperature and impregnation ratio are relatively independent.

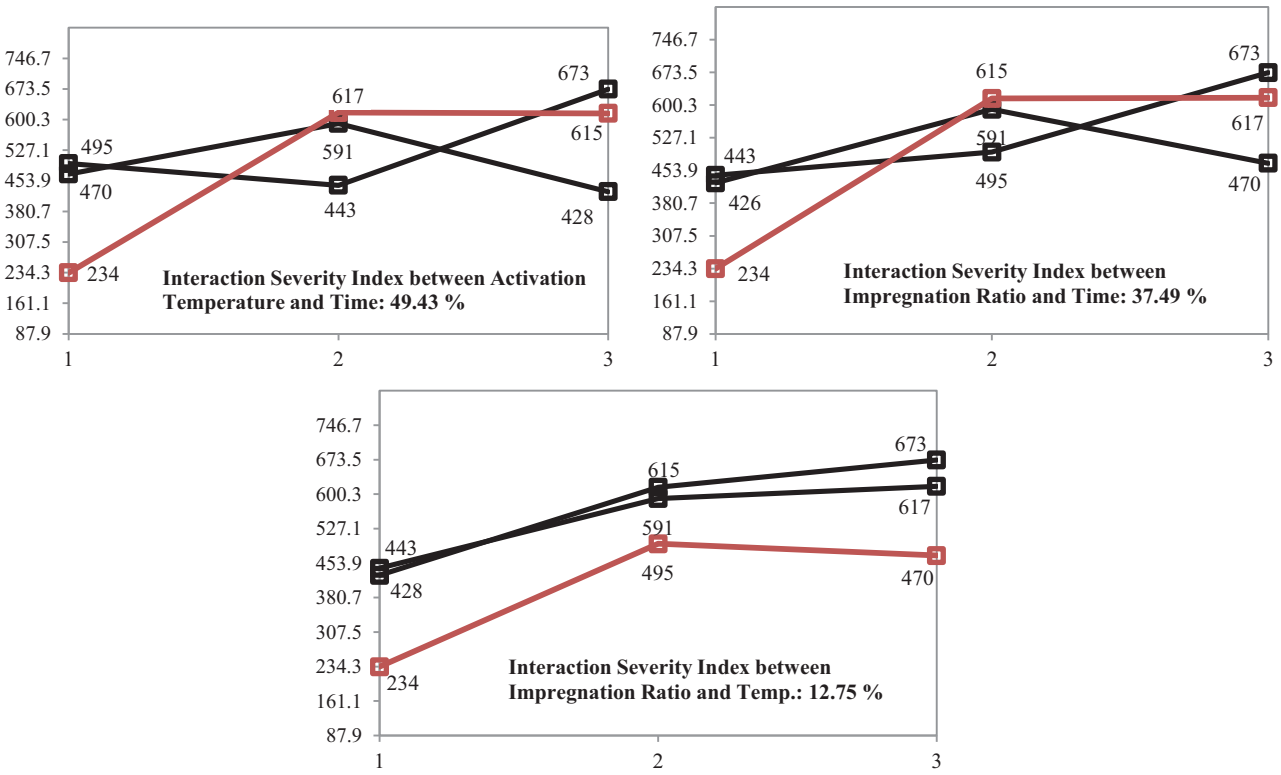

Figure 2. Interaction severity index between pairs of factors in activation tests.

The activated carbon production yield was approximately 30%, which is close to the value obtained by Elwakeel et al. (27%).[12] Typical reported yields by Castro et al. were 35%–46%.[14] In complementary tests, optimization of the operating conditions to reach the highest yield was also performed. According to Figure 1b, increasing the activation time and temperature both decrease the production yield due to gasification of much more carbonaceous material. In contrast, larger impregnation ratios (in the range studied) led to yield increasing; however, using much higher amounts of chemical activators due to promoting the macro- and mesoporosity and gasification of carbon may lead to loss of yield. In the present work, the contribution percentage of this parameter on the production yield was only about 4% compared to temperature and time with percentages of 62% and 32%, respectively. The SI values were as follows: [impregnation ratio × time]: 47.32%, [temperature × time]: 13.63%, and [impregnation ratio × temperature]: 5.08%. Finally, the optimal conditions to obtain adsorbent

with the largest production yield (47.72%) were impregnation ratio: 1.5, activation temperature: 350 °C, and time of activation: 0.5 h.

2.2. Adsorbent characterization results

The multipoint specific surface area and the total pore volume of the optimized bagasse-based activated carbon were calculated as 972.5 m^2/g and 0.82 cm^3/g, respectively; the proportion of microporosity in the total pore volume was approximately 52% (micropore volume: 0.43 cm^3/g). The mean pore width (diameter) was also measured as equal to 33 Å, confirming the presence of mesopores with widths of greater than 20 Å. The porous properties of activated carbons synthesized from bagasse reported in the literature are also gathered in Table 2 for comparison. The data show that the type of chemical activator has a great influence on the porosity and pore size distribution of activated carbons produced from the same kind of precursor. Among the most common chemical agents, $ZnCl_2$ and H_3PO_4 act as dehydrating agents; however, KOH acts as an oxidant.[31] The dehydrating chemicals eliminate the water available in the structure of precursors and thus prevent the formation of tar that could clog the pores.

Table 2. Comparison of porous properties of activated carbon prepared from chemical/physical activation of sugarcane bagasse.

Powdered ACs prepared from bagasse using different activating agents	BET surface area (m^2/g)	Total pore volume (cm^3/g)	Micropore volume (cm^3/g)	Average pore width (Å)	Reference
Sugarcane bagasse / $ZnCl_2$	864	0.43	0.44	20.5	[25]
Bagasse / KOH	2299	1.45	0.91	25.3	[32]
Bagasse / steam physical activation	607	0.45	0.31	29.4	
Bagasse / $ZnCl_2$	717	-	-	31	[4]
Bagasse / H_3PO_4	129	-	-	56	
Sugarcane bagasse / H_3PO_4	1132	1.12	0.61	19.8	[14]
Sugarcane bagasse / H_3PO_4	671.54	0.426	-	13.0	[12]
Sugarcane bagasse / H_3PO_4	320	1.234	0.43	-	[11]
Carbonized sugarcane bagasse / H_3PO_4	557	0.583	0.273	-	[5]
Sugarcane bagasse / H_3PO_4	1236	-	0.17	34.24	[29]
Sugarcane bagasse / H_3PO_4	972.5	0.82	0.43	33	Present work

In the chemical activation of bagasse, KOH has led to a larger surface area compared to the other chemical activators; it is worth noting that relatively higher temperatures (>700 °C) and impregnation ratios were applied in the work.[32] It is established in many works that KOH activation leads to activated carbons with greater specific surface area and good (micro)pore development compared to other ones.[33] This is related to the liberation of CO or CO_2 gases produced inside the structure of the precursor during the activation. The successive reactions involved consist of KOH dehydration into K_2O, and K_2O reaction with CO_2 leading to formation of K_2CO_3.[27,34] Usually at temperatures higher than 700 °C, KOH or any of its products as K_2CO_3 will be reduced to metallic potassium. The presence of metallic ions acts as a catalyst and accelerates the carbon liberation and so creates a larger surface area, high pore volume, and lower production yield.[33]

Activation with H_3PO_4 occurs via dehydration and decomposition of the organic material, which reduces the dimension of particles; however, the presence of chemical reactants inside the particles' structure inhibits the reduction to some extent. This can be conducted by the formation of linkages/bridges such as phosphate and polyphosphate esters connecting the biopolymers.[8,31,35] It is found that $ZnCl_2$ usually leads to higher surface areas and smaller pores with higher uniformity compared to H_3PO_4 under similar conditions. This is related to the small size of the $ZnCl_2$ molecules or its hydrates penetrating inside the precursor structure. In contrast, H_3PO_4 leads to mesoporous activated carbons with much nonuniformity. The presence of a mixture of molecules with varying dimensions from small H_3PO_4 and $H_4P_2O_5$ to large $H_{13}P_{11}O_{34}$ may be the reason.[31,34]

SEM micrographs of the activated bagasse in comparison with the raw one are shown in Figure 3. It is obvious that activation is accompanied by significant changes in the size and number of pores.

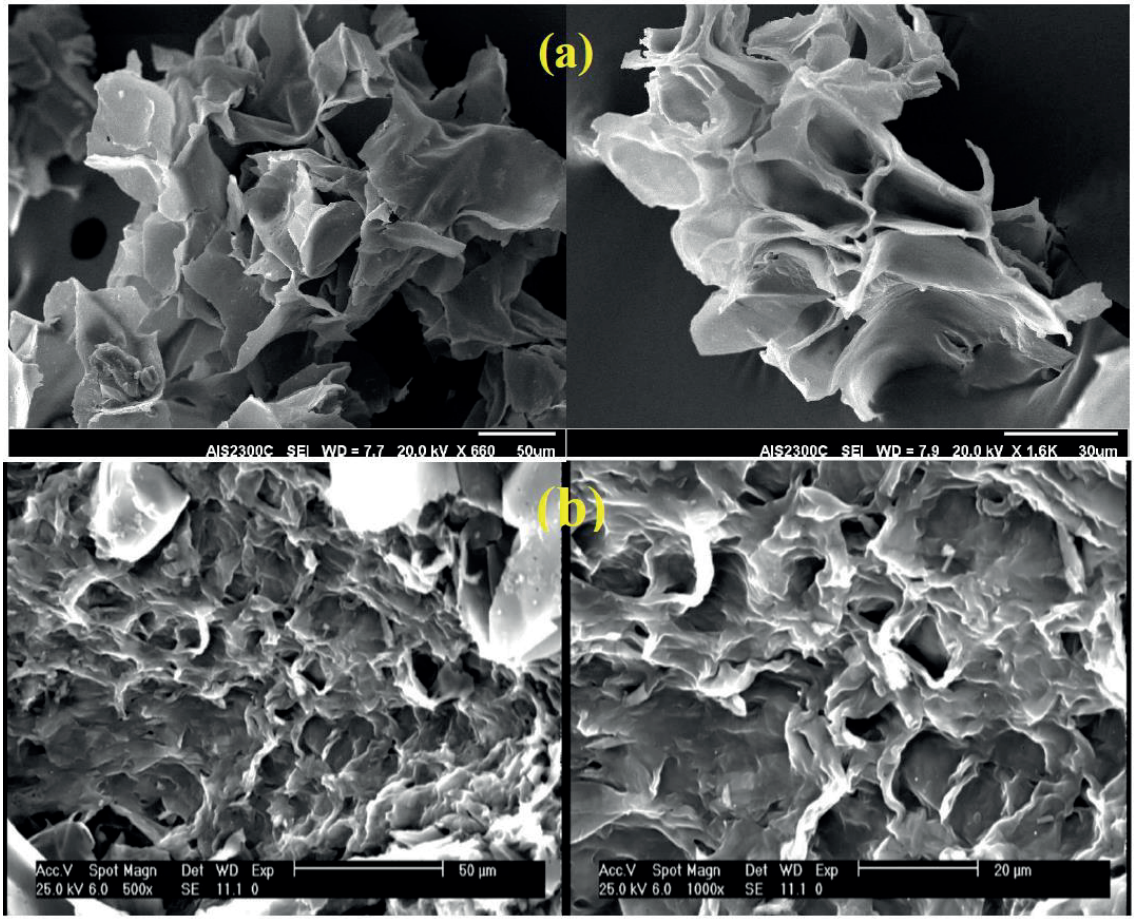

Figure 3. SEM micrographs of (a) raw sugarcane bagasse in comparison with (b) H_3PO_4-activated carbon prepared from bagasse.

Considering the kinetic diameter of phenol molecules (~6.7 Å), micropores (up to 20 Å) could act as the main sites for trapping and physical adsorption of phenol species. Juang et al. confirmed that phenol adsorption in microporous adsorbents occurs with more efficiency than the other types.[36] Thus, it is estimated that the bagasse-based sample with about 52% microporosity gives a moderate phenol adsorption capacity.

Figure 4 shows the FTIR spectra of the bagasse-based activated carbon and the raw material comparatively. Both spectra showed similar peaks in the range of 2500–4000 cm^{-1}; a broad strong peak at 3400 cm^{-1} represented the stretching O–H bond in phenolic and carboxylic functional groups and also adsorbed water; the activated carbon showed a greater peak than the raw material. C–H stretching bonds lead to vibrations around 2900 cm^{-1} and 1450 cm^{-1}; the amounts of this group decreased after the activation because of carbon burning and its liberation in the forms of oxidized carbons. C=O bonds available in the structure of ketones, aldehydes, lactones, or carboxyl groups produce small peaks at around 1700 cm^{-1}. The vibrations at 1590 cm^{-1} are also attributed to the C–C vibrations in the aromatic rings. For the raw bagasse, vibrations in the range of 1000–1300 cm^{-1} are simply related to C–O stretching in acids, alcohols, phenols, ethers, and/or esters groups. However, for H_3PO_4-activated bagasse, the presence of phosphorous-containing groups may cause a small change in the location of the peaks mentioned above and overlapping of the bonds. The phosphorous-containing bonds such as P=O, P–O–C, and P=OOH are probably available in the structure of the H_3PO_4-activated carbon.[37,38]

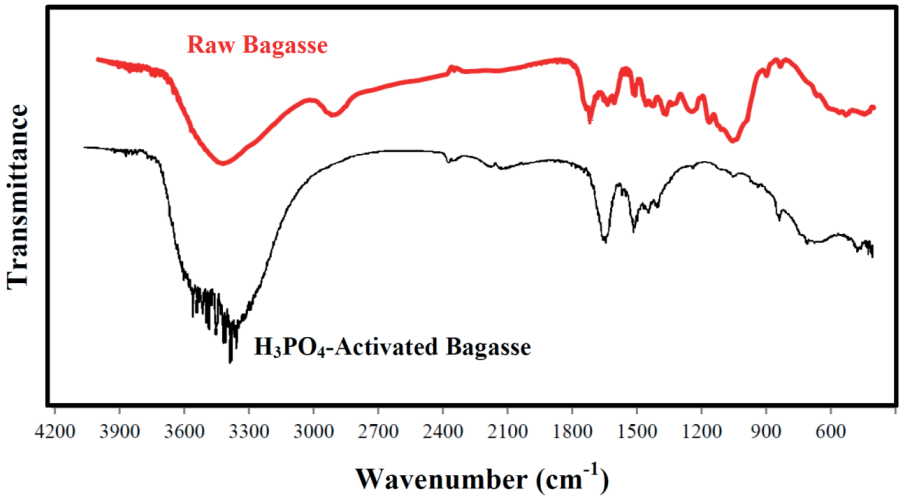

Figure 4. The FTIR spectra of raw and H_3PO_4 activated carbon.

CHN/O elemental analysis of the bagasse-based adsorbent showed the following percentages: carbon: 69.13%, hydrogen: 2.36%, nitrogen: 0.29%, and oxygen: 28.22% (estimated by difference), in comparison with the average weight percentages of the raw bagasse (carbon: 46.9%, hydrogen: 6.3%, nitrogen: 1.2%, and oxygen: 45.6%). Hydrogen decreasing after activation confirmed the FTIR results. Carbon enrichment after the activation is associated with the liberation of oxygen, hydrogen, and nitrogen, remaining a carbon-rich structure.

2.3. Phenol adsorption results

The kinetic experimental results (Figure 5: q_t (mg/g) vs. t (min)) showed that the adsorbent could reach over 95% of its final equilibrium capacity after only 30 min. In comparison with most commercial adsorbents with slow uptake rates (Table 3), such a short equilibrium time can be taken into account as one of the benefits of using this kind of adsorbent in industrial applications and real environments. It seems that the final adsorption capacity of the bagasse-based activated carbon is approximately 27 mg/g, which is three times larger than the value reported by Srivastava et al. for the equilibrium adsorption capacity of bagasse fly ash at the

initial concentration of 100 mg/L.[21] In order to estimate the efficiency of the proposed procedure, a relatively comprehensive literature review was conducted of the studies that worked on activation of agricultural/industrial wastes and used the produced adsorbent for phenol adsorption. The results are summarized in Table 3. All the factors influencing the kinetic experimental results, including the particle size and agitation rate, are gathered and thus comparison of the equilibrium time is possible. It can be seen that one of the shortest equilibrium times is that of the bagasse-activated carbon prepared in the present work. It can be observed that that the average particle size of the sorbent is larger than the others (850–1700 µm); however, the shaking speed is relatively higher. Activated carbons produced from phosphoric acid activation of corn cobs with the smaller particle size of 150–430 µm were among the other fast adsorbents with equilibrium time of 20 min under an agitation rate of 100 rpm.[39] $ZnCl_2$ activated coir pith carbon particles with average particle size of 250–500 µm had an equilibrium time of 10–25 min with the agitation rate of 200 rpm.

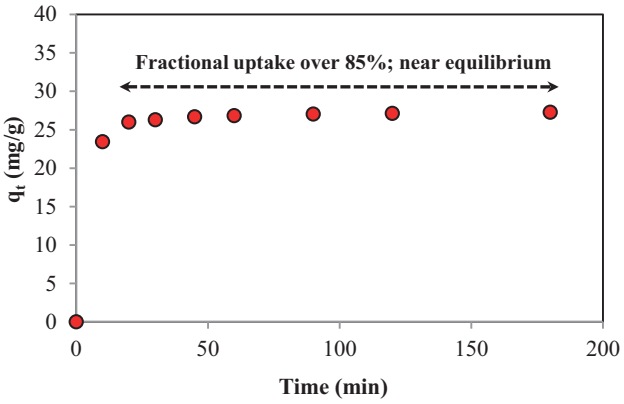

Figure 5. The kinetic experimental data of phenol adsorption.

Table 3. Comparison of the time required to reach equilibrium for phenol adsorption from dilute aqueous solutions using different biomass-based ACs.

Activated carbon from ...	Particle size (µm)	Temperature	Agitation speed (rpm)	Equilibrium contact time	The best pH range	Reference
Tea waste	< 150	Room temp.	400	>100 min	4–8	[40]
Rattan sawdust	150	30 °C	120	150 min	3–8	[41]
Lantana camara	HCl: 11.59 KOH: 11.68	25 °C	140	6 h 70 h	4–8	[42]
Corn cobs	150–430	Room temp.	100	20 min	-	[39]
Eucalyptus wood	PAC: 297–420 Extrude: D: 4000; H: 7000	25 °C	100	>500 min >1500 min	-	[43]
Coir pith	250–500	35 °C	200	10–25 min	2–8	[44]
Banana peels	250–500	25 °C	150	60 min	4–8	[45]
Bagasse	850–1700	Room temp.	300	< 30 min	4–8	Present work

Figure 5 shows that the fractional adsorption (q_t/q_e) reaches 86% after only 10 min. Thus, performing more quantitative evaluations to predict a descriptive kinetic model may not be necessary. Furthermore, based on the previous work, using the kinetic data with fractional uptake over 85% may cause selection of incorrect and unreliable chemical kinetic models.[46]

The adsorption optimization tests and ANOVA analysis (Table 4) showed that among the influencing factors including phenol concentration, pH of the solution, and adsorbent dosage, the largest contribution was about 82.521%, which belonged to the concentration. According to this table, the initial pH of the solution does not have a significant influence on the response; however, the other factors are meaningful with significance of over 90% and 99.99%. Figure 6 shows that the higher concentrations lead to higher adsorption capacities, due to the larger driving force provided for adsorption onto empty sites. As expected from the formula ($q = \frac{V(C_0 - C)}{m}$), higher adsorbent dosage (m) results in lower adsorption capacity (q), with a contribution of about 12%. This behavior may be due to the high resistance against the adsorbate penetration caused by the accumulation of adsorbent particles.

Table 4. Results of the analysis of the variance (ANOVA table) for phenol adsorption.

Factor	DOF (f)	Sum of squares (S)	Variance (V)	F-ratio (F)	Significance	Percent (%)
Initial pH of solution	2	51.447	25.723	4.817	< 90.00%	3.083
Initial concentration	2	1100.812	550.406	103.087	>99.99%	82.436
Adsorbent dosage	2	159.446	79.723	14.931	>90.00%	11.249
Other/error	2	10.677	5.338			3.232
Total	8	1322.384				100.00%

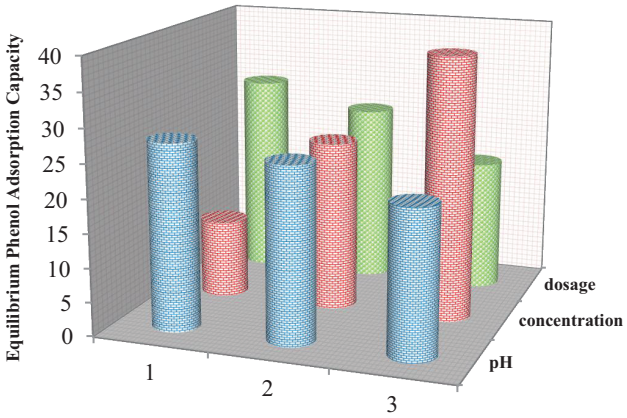

Figure 6. The influence of adsorption parameters on the equilibrium phenol adsorption capacity of bagasse-based AC; 1, 2, and 3 represent the corresponding levels of each factor in the Taguchi design.

The initial pH of solution showed a smaller descending influence (3.282%) on the adsorption capacity towards phenol in the range studied (4–8). According to Visual MINTEQ, an equilibrium speciation model (US Environmental Protection Agency), over the extensive range of pH up to 8, phenol exists only as C_6H_5OH (unionized acidic compound). Acidic medium (pH < 7) promotes phenol protonation and makes them attractive species for being adsorbed onto the negative oxygenated groups available on the surface of adsorbent at pH >pH_{pzc}. The point of zero charge for the bagasse-based adsorbent activated with phosphoric acid was measured at around 4, so over the whole range studied (4 < pH < 8), the adsorbent surface possesses negative charge and it is appropriate for adsorption of protonated phenol. The largest capacity belongs to pH 4 and it decreases slightly increasing the solution pH up to 8. At higher values (pH >8), phenol dissociates to produce phenolate anion ($C_6H_5O^-$) and the affinity between this compound and the negative surface is expected to be reduced.

Most studies in Table 3 confirm these results; the optimal pH range for phenol adsorption is reported between 4 and 8. Considering the ignorable influence of pH on the adsorption capacity, pooling this factor increased the error percentage from 2.474% only to 5.76%, with new percentages of 82.52% and 11.72% for concentration and dosage, respectively. Finally the optimal conditions to reach the highest adsorption capacity were determined: the initial concentration (200 ppm), adsorbent dosage (1 g/L), and solution pH (4). The value predicted by the Taguchi model (45.84 mg/g) was comparable to the real one (42.90 mg/g) measured experimentally under the same conditions, and the error percentage was around 6%. The most important interaction was also observed between the initial solution pH and adsorbent dosage. Due to the intrinsic surface charge, the existence of adsorbents in solutions can affect the solution pH, and this is the reason for such high interaction. In contrast, smaller interactions were observed between [concentration × dosage] and [pH × concentration].

For quantitative evaluation of the equilibrium data, three of the most common isotherm models including the Langmuir, Freundlich, and Dubinin–Radushkevich were applied. These models are able to describe adsorption from dilute aqueous solutions onto strong adsorbents very well. For phenol adsorption especially onto carbonaceous adsorbents, many researchers reported the good correspondence of equilibrium results with these models (Table 5). For the bagasse-based adsorbent prepared in the present work and phenol-contaminated water with initial concentration of 50–350 ppm, the correspondence of isotherm data with the nonlinear equations of these models was assessed (Figure 7). R^2 and RMSE values showed that there is no preference between the Langmuir and Freundlich models to fit the laboratory data, and both are sufficiently good (Table 6). Therefore, probably the concentration range studied is not sufficient for reflecting the differences of these models and deciding whether there is a monolayer adsorption or a variety of sorption sites.

The Dubinin–Radushkevich model gives an estimation of the energy and nature of adsorption.[47] This model fit the data much better, regarding the lower RMSE and higher R^2 values (Table 6). One of the factors that can be extracted from Dubinin–Radushkevich model is the apparent adsorption energy (E), estimating the kind of adsorption. Values lower than 8 kJ/mol are attributed to physical adsorption; however, energies in the range of 8 to 16 kJ/mol are related to ion exchange and weak chemical adsorption mechanisms.[48] Table 6 indicates that the magnitude of E for the current work equals 10.94 kJ/mol, which is in the rage of ion-exchange mechanisms.

2.4. Conclusions

For chemical activation of sugarcane bagasse with H_3PO_4, the most important factors affecting the iodine number of the produced activated carbons were the impregnation ratio and temperature of activation with contribution percentages of 60 and 36%, respectively. The highest interaction was found between time and two other factors. The best temperature for activation of bagasse with H_3PO_4 was 550 °C and heating for 30 min led to higher yields. H_3PO_4 activation under the optimal conditions resulted in a micromesoporous activated carbon (50/50) with mean pore width of 33 Å, which can act as a relatively efficient phenol adsorbent. In the range studied for the initial phenol concentration, both the Langmuir and Freundlich models fit the equilibrium data equally well; however, the correspondence with the Dubinin–Radushkevich model was much better. Based on the adsorption energy parameter calculated from the Dubinin–Radushkevich model and the pH dependency of adsorption capacity, the mechanism of phenol adsorption is not limited to the physisorption and weak physical interactions, and the role of the ion-exchange mechanism and electrostatic interactions is significant.

Table 5. The best-fit isotherms and the related parameters for equilibrium phenol adsorption onto different biomass-based ACs.

Activated carbon from ...	Initial concentration (ppm)	Adsorbent dosage (g/L)	Isotherm models*			Reference
			The best-fit model	The 2nd best-fit model	The 3rd best-fit model	
Tea waste	100–1000	2	L: q_{max} = 142.9	F: K_F = 17.21	-	[40]
Rattan sawdust	25–200	-	L: q_{max} = 149.25	DR: q_s = 22.99 E = 0.707	F: K_F = 29.37	[41]
Lantana camara	25–250	0.75 1	L: q_{max} = 112.5 L: q_{max} = 91.07	F: K_F = 1.35 F: K_F = 1.33	DR: q_s = 60; E = 0.1582 DR: q_s = 46; E = 0.2425	[42]
Corn cobs	100–500	10	F: K_F = 3.91	L:q_{max} = 52.3	-	[39]
Eucalyptus wood	10–500	1	L:q_{max} = 64 L: q_{max} = 4	F: K_F = 0.6 F: K_F = 0.6	-	[43]
Coir pith	40–120	2	DR: q_s = 589.8; E = 9.13	F: K_F = 5.87	L: q_{max} = 92.59	[44]
Banana peels	50–500	6	F: K_F = 2.01	L: q_{max} = 80.65	-	[45]
Bagasse	50–350	2	DR: q_s = 194.34; E = 10.94	L: q_{max} = 68.89	F: K_F = 3.86	Present work

*L: Langmuir [q_{max} (mg/g)], F: Freundlich [K_F (mg/g) $(L/mg)^{1/n}$];
DR: Dubinin–Radushkevich [q_s (mg/g) & E (kJ/mol)].

Table 6. The equilibrium parameters of phenol adsorption onto the bagasse-based AC.

Langmuir $\left(q_e=\frac{q_{max}K_Lc_e}{1+k_Lc_e}\right)$	Freundlich $\left(q_e= K_f c_e^{1/n}\right)$	Dubinin–Radushkevich $\left(\begin{array}{l} q_e= q_s exp(-K_{DR}e^2) \\ e = RTln(1+\frac{1}{c_e}) \\ E = \frac{1}{\sqrt{2K_{DR}}} \end{array}\right)$
q_{max} = 68.89 mg/g	K_f = 3.864 [mg/g $(L/mg)^{1/n}$]	q_s = 0.0034 mol/g = 344. 72 mg/g
K_L = 0.01389 L/mg	$1/n$ = 0.4935	$K_{DR} = 4.18 \times 10^{-9}$ $(mol/J)^2$
R^2 = 0.9944	R^2 = 0.9943	R^2 = 0.9966
RMSE = 1.252	RMSE = 1.257	RMSE = 9.77×10^{-6}

3. Experimental

3.1. Preparation of activated carbon

In the current research, sugarcane bagasse supplied from a local sugar mill in the south of Iran, Karoon Company, was applied accordingly to produce porous adsorbent:

(I) Predrying of bagasse stacks by exposure to direct sunlight for 7 days;

(II) Chipping and sieving of dried bagasse to obtain the desired range of particle size: 0.85 mm–1.70 mm;

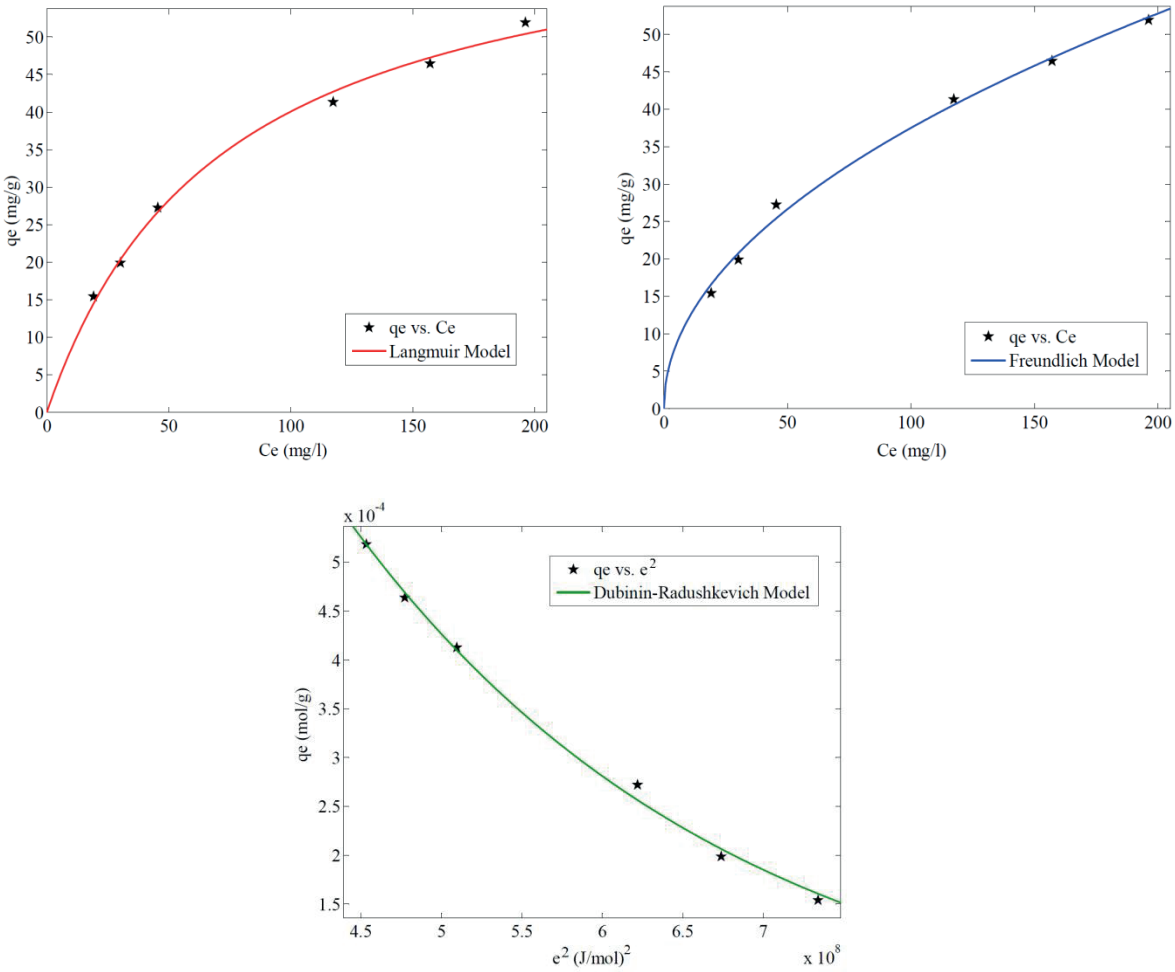

Figure 7. The equilibrium adsorption data fitted with nonlinear forms of the Langmuir, Freundlich, and Dubinin–Radushkevich isotherm models.

(III) Impregnation of a weighed amount of bagasse in H_3PO_4 solution (Merck, 85 wt.%) at 90 °C and agitation for 15 h; distilled water was added in this step for better mixing (water to bagasse weight ratio: 10/1);

(IV) Exposure of the solidified impregnated mixture to heat treatment in an adjustable muffle furnace under the self-generated atmosphere, where heating rate to reach the final temperature was considered at about 2.5 °C/min;

(V) Cooling of the activated material to room temperature slowly, weighing and then washing with hot distilled water to remove any unreacted chemical agent and phosphates that remained in the structure of adsorbent; washing continues until the pH of the filtrate reaches the pH of distilled water;

(VI) The final step includes drying the adsorbent at 110 °C for 5 h, weighing it, and storing it in air-tight containers.

Among all the parameters influencing the activation performance (for example, impregnation temperature, rate of temperature rise, atmosphere used in the furnace), three were chosen as key parameters.[10,14,27,49] These

parameters accompanied by their different levels are as follows and the overall ranges of the operating conditions were selected based on previous studies:[13,14,29,50]

(I) 0.25, 0.75, and 1.5 wt./wt. for the impregnation ratio;

(II) 350, 450, and 550 °C for the activation temperature;

(III) 0.5, 1, and 2 h for the activation time.

In order to achieve the optimal conditions and examine the relative influence of production parameters on the efficiency and their possible interactions, the Taguchi procedure and L_9 orthogonal array were applied by Qualitek-4 program.

1. **Characterization of activated carbon**

A series of characterization tests were performed to determine several important porous and physicochemical properties of the bagasse-based adsorbent. First of all, activated carbon production yield was calculated by dividing the weight of washed/dried adsorbent product by the weight of dried raw material. The iodine number of the adsorbent as an index representing the activity level and micropore content was measured according to the standard method of ASTM D 4607-94.[51] A higher iodine number indicates a higher degree of activation. The specific surface area and micropore volume were determined respectively by applying BET and HK equations on the isotherms of N_2 physical adsorption-desorption at 77 K obtained with a Quantachrome NOVA Series 1000 volumetric adsorption analyzer. Average pore size was computed using the $4V_{tot}$/SBET equation, with the assumption that the pores are cylindrical. The overall pore volume (V_{tot}) was predicted from the concentration of nitrogen adsorbed at the highest relative pressure. SEM micrographs of the raw material and activated carbon produced were also prepared with a Philips XL30 scanning electron microscope. The functional groups available on the surface of the sorbent and the raw material were determined based on the FTIR spectroscopy method (Thermo Scientific, Nicolet). CHN/O elemental analysis was carried out for measuring the percentages of elements in the adsorbent's bulk (PerkinElmer). The pH drift technique was used to determine pH_{pzc} (point of zero charge) by agitating electrolyte NaCl solutions (0.1 M) with the adsorbent dosage of 150 mg per 50 mL of solution under a wide range of initial pHs.[52]

1. **Phenol adsorption experiments**

In order to perform each adsorption test in batch mode, the suspension containing phenol solution and adsorbent particles with the predetermined initial concentration and dosage was shaken at a speed of 300 rpm at room temperature. A minimum amount of HCl and/or NaOH solution (0.1 N) was applied to adjust the initial pH. The measurement of phenol concentration in solutions (in the range of ppm) was performed with a UV/VIS spectrophotometer at a wavelength of 269 nm. Three series of adsorption experiments including kinetic, isotherm, and optimization tests were performed:

(I) Kinetic tests were carried out to reach the equilibrium time for phenol uptake under the following operating conditions: initial concentration of phenol: 100 ppm, adsorbent dosage: 2 g/L, initial solution pH: 4, and a range of agitating time between 10 min and 3 h (10, 20, 30, 45, 60, 90, 120, and 180 min).

(II) Equilibrium tests were performed to recognize the best-fit adsorption isotherm model under the conditions: adsorbent dosage: 2 g/L, initial pH: 4, agitation time: 24 h, and phenol concentrations between 50 and 350 ppm (50, 70, 100, 150, 200, 250, 300, and 350 ppm).

(III) The Taguchi procedure was applied to study the influences and interactions of three effective adsorption parameters on the capacity of AC. The selected factors and their varying levels were: (I) initial solution pH: 4, 6 and 8; (II) initial phenol concentration: 50, 100 and 200 ppm; and (III) adsorbent dosage: 1, 2 and 3 g/l.

References

1. Yahya, M. A.; Al-Qodah, Z.; Ngah, C. W. Z. *Renew. Sust. Energ. Rev.* **2015**, *46*, 218-235.
2. Giusto, L. A. R.; Pissetti, F. L.; Castro, T. S.; Magalhães, F. *Water Air Soil Poll.* **2017**, *228*, 1-11.
3. Tran, V. T.; Quynh, B. T. P.; Phung, T. K.; Ha, G. N.; Nguyen, T. T.; Bach, L. G. *Journal of Undergraduate Science & Technology* **2016**, *54*, 277-284.
4. Syna, N.; Valix, M. *Mineral Eng.* **2003**, *16*, 511-518.
5. Mohamed, E. F.; El-Hashemy, M. A.; Abdel-Latif, N. M.; Shetaya, W. H. *J. Air Waste Manag. Assoc.* **2015**, *65*, 1413-1420.
6. Gardare V. N.; Yadav, S.; Avhada, D. N; Rathod, V. K. *Desalin. Water Treat.* **2014**, *2014*, 1-7.
7. Kumar, A.; Jena, H. M. *Results Phys.* **2016**, *6*, 651-658.
8. Xu, J.; Chen, L.; Qu, H.; Jiao, Y.; Xie, J.; Xing, G. *Appl. Surf. Sci.* **2014**, *320*, 674-680.
9. Satyawali, Y.; Balakrishnan, M. *Bioresour. Technol.* **2007**, *98*, 2629-2635.
10. Soleimani, M.; Kaghazchi, T. *Chem. Eng. Technol.* **2007**, *30*, 649-654.
11. Giraldo-Gutiérrez, L.; Moreno-Piraján, J. C. *J. Anal. Appl. Pyrol.* **2008**, *81*, 278-284.
12. Elwakeel, K. Z.; El-Sayed, G. O.; Abo El-Nassr, S. M. *Desalin. Water Treat.* **2015**, *55*, 471-483.
13. Adib, M. R. M.; Suraya, W. M. S. W.; Rafidah, H.; Amirza, A. R. M.; Attahirah, M. H. M. N.; Hani, M. S. N. Q.; Adnan, M. S. *IOP Conf. Ser. Mater. Sci. Eng.* **2016**, *136*, 1-9.
14. Castro, J. B.; Bonelli, P. R.; Cerrella, E. G.; Cukierman, A. L. *Ind. Eng. Chem. Res.* **2000**, *39*, 4166-4172.
15. Asadi-Kesheh, R.; Mohtashami, S. A.; Kaghazchi, T.; Asasian, N.; Soleimani, M. *Sep. Sci. Technol.* **2015**, *50*, 223-232.
16. Adib, M. R. M.; Attahirah, M. H. M. N.; Amirza, A. R. M. *IOP Conference Series Earth and Environmental Science* **2018**, *140*, 012029.
17. Molva, M. MSc, İzmir Institute of Technology, İzmir, Turkey, 2004.
18. Nageeb Rashed, M. In *Organic Pollutants - Monitoring, Risk and Treatment*; Nageeb Rashed, M., Ed. InTech Publisher: Rijeka, Croatia, 2013, pp. 167-194.
19. Kamel, S.; Abou-Yousef, H.; Yousef, M.; El-Sakhawy, M. *Polymers* **2012**, *88*, 250-256.
20. Gupta, V. K., Sharma, S.; Yadav, I. S.; Mohan, D. *J. Chem. Technol. Biotechnol.* **1998**, *71*, 180-186.
21. Srivastava, V. C.; Swamy, M. M.; Mall, I. D.; Prasad, B.; Mishra, I. M. *Colloids Surf. A Physicochem. Eng. Asp.* **2006**, *272*, 89-104.
22. Srivastava, V. C.; Prasad, B.; Mishra, I. M.; Mall, I. D.; Swamy, M. M. *Ind. Eng. Chem. Res.* **2008**, *47*, 1603-1613.
23. Karunarathne, H. D. S. S.; Amarasinghe, B. M. W. P. K. *Energy Procedia* **2013**, *34*, 83-90.

24. Mukherjee, S.; Kumar, S.; Misra, A. K.; Fan, M. *Chem. Eng. J.* **2007**, *129*, 133-142.
25. Kalderis, D.; Koutoulakis, D.; Paraskeva, P.; Diamadopoulos, E.; Otal, E.; Olivares del Valle, J.; Fernández-Pereira, C. *Chem. Eng. J.* **2008**, *144*, 42-50.
26. Roy, R. A *Primer on the Taguchi Method*; Van Nostrand Reinhold: New York, NY, USA, 1990.
27. Marsh, H.; Rodriguez-Reinoso, F. *Activated Carbon*; Elsevier Science & Technology Books: London, UK, 2006.
28. Kaghazchi, T.; Asasian Kolur, N.; Soleimani, M. *J. Ind. Eng. Chem.* **2010**, *16*, 368-374.
29. Mendes, F. M. T.; Marques, A. C. C.; Mendonc, D. L.; Oliveira, M. S.; Moutta, R. O.; Ferreira-Leitao, V. S. *Waste Biomass Valor.* **2015**, *6*, 433-440.
30. Montgomery, D. C. *Design and Analysis of Experiments*; John Wiley & Sons: New York, NY, USA, 2011.
31. Zhou, W.; Liu, X.; Zhou, K.; Jia, J. In *Nanomaterials in Advanced Batteries and Supercapacitors*; Ozoemena, K. I.; Chen, S., Eds. Springer International Publishing: Basel, Switzerland, 2016, pp. 271-315.
32. Tseng, R. L.; Tseng, S. K. *J. Hazard. Mater.* **2006**, *136*, 671-680.
33. Hui, T. S.; Ahmad Zaini, M. A. *Carbon Lett.* **2015**, *16*, 275-280.
34. Molina-Sabio, M.; Rodriguez-Reinoso, F. *Colloids Surf. A Physicochem. Eng. Asp.* **2004**, *241*, 15-25.
35. Enaime, G.; Ennaciri, K.; Ounas, A.; Baçaoui, A.; Seffen, M.; Selmi, T.; Yaacoubi, A. *J. Mater. Environ. Sci.* **2017**, *8*, 4125-4137.
36. Juang, R. S.; Tseng, R. L.; Wu, F. C. *Adsorption* **2001**, *7*, 65-72.
37. Yakout, S. M.; Sharaf El-Deen, G. *Arab. J. Chem.* **2016**, *9*, S1155-S1162.
38. Pavia, D. L.; Lampman, G. M.; Kriz, G. S.; Vyvyan, J. A. *Introduction to Spectroscopy*; Brooks/Cole: Belmont, CA, USA, 2008.
39. Rocha, P. D.; Franca, A. S.; Oliveira, L. S. *International Journal of Engineering & Technology* **2015**, *7*, 459-464.
40. Gundogdu, A.; Duran, C.; Basri Senturk, H.; Soylak, M.; Ozdes, D.; Serencam, H.; Imamoglu, M. *J. Chem. Eng. Data* **2012**, *57*, 2733-2743.
41. Hameed, B. H.; Rahman, A. A. *J. Hazard. Mater.* **2008**, *160*, 576-581.
42. Girish, C. R.; Ramachandra Murty, V. *Int. Sch. Res. Notices* **2014**, *2014*, 1-16.
43. Tancredi, N.; Medero, N.; Möller, F.; Píriz, J.; Plada, C.; Cordero, T. *J. Colloid Interface Sci.* **2004**, *279*, 357-363.
44. Subha, R.; Namasivayam, C. *Can. J. Civ. Eng.* **2009**, *36*, 148-159.
45. Ingole, R. S.; Lataye, D. H.; Dhorabe, P. T. *KSCE J. Civ. Eng.* **2017**, *21*, 100-110.
46. Simonin, J. P.; *J. Chem. Eng.* **2016**, *300*, 254-263.
47. Carrasco-Marin, F.; Lopez-Ramon, M. V.; Moreno-Castilla, C. *Langmuir* **1993**, *9*, 2758-2760.
48. Wu, X. W.; Ma, H. W.; Li, J. H.; Zhang, J.; Li, Z. H. *J. Colloid Interface Sci.* **2007**, *315*, 555-561.
49. Madadi Yeganeh, M.; Kaghazchi, T.; Soleimani, M. *Chem. Eng. Technol.* **2006**, *29*, 1247-1251.
50. Taha, N. A.; Abdelhafez, S. E.; El-Maghraby, A. *Global NEST Journal* **2016**, *18*, 402-415.
51. ASTM. *Standard, Designation D4607-94, Standard Test Method for Determination of Iodine Number of Activated Carbon*; ASTM: West Conshohocken, PA, USA, 2000.
52. Lopez-Ramon, M. V.; Stoeckli, F.; Moreno-Castilla, C.; Carrasco-Marin, F. *Carbon* **1999**, *37*, 1215-1221.